



The relationship between atmospheric blocking and precipitation changes in Turkey between 1977 and 2016

Bahtiyar Efe^{1,2} · Anthony R. Lupo² · Ali Deniz¹

Received: 22 December 2018 / Accepted: 10 May 2019 / Published online: 18 June 2019
© Springer-Verlag GmbH Austria, part of Springer Nature 2019

Abstract

The relationship between blocking events and mean precipitation frequency (MPF) was investigated in this work for Turkey during 1977–2016. The overall MPF for the examined stations during blocked days (nonblocked days) fluctuated between 0.15 and 0.43 (0.12 and 0.38). The ratio of MPF during the blocked days to nonblocked days ranges between 12 and 38%. During the winter season, the country has higher MPF values during blocked days. The greatest ratio of MPF values during blocked days to nonblocked days is observed in summer due to smaller values of MPF occurring during this season overall. Higher MPF occurs when the event center was located between 0° and 30° E (mean 0.27, range 0.17–0.51). There is no relationship between blocking duration and MPF for all seasons. There is a positive relationship between blocking intensity and MPF during summer (CC = 0.35, significant at the 95% level) and fall (CC = 0.43, significant at the 95% level). The relationship between blocking longitudinal extent and MPF is significant at the 95% confidence level during the summer and fall seasons with correlation coefficients of 0.29 and 0.25, respectively. A composite of the 10 blocking events associated with the largest MPF demonstrated that there is moist advection via westerly flow into Turkey in all seasons. During winter, a greater proportion of these events is observed during the La Niña phase of El Niño Southern Oscillation, but during El Niño in spring and summer. For the blocking case study (31 October to 5 November 2009) associated with the largest MPF, the mean value across the country was 0.73. The mean total precipitation during this period was 63.4 mm.

1 Introduction

Atmospheric blocking events, which can be described as the “stagnation of air parcels over the same region during a long period of time,” are an important phenomenon that causes extreme events like cold spells (O’Reilly et al. 2016; Aalijahan et al. 2018; Brunner et al. 2018), heat waves (Sitnov et al. 2014; Demirtaş 2018; Lhotka et al. 2018), and heavy precipitation (Khodayar et al. 2018; Rabinowitz et al. 2018). Also, blocking events have been examined by researchers focusing on the relationship between these events and teleconnection patterns (Luo et al. 2007a, b; Lupo et al. 2017), predictability (Bengtsson 1981;

Tibaldi and Molteni 1990 (*hereafter* TM90); Matsueda 2011), defining the blocking indicators or its characteristics (Lejenas and Okland 1983; TM90; Lupo and Smith 1995; Barriopedro et al. 2006), or the influence of these events on regional climate (Antokhina et al. 2016; Whan et al. 2016; Nunes et al. 2017; Sitnov et al. 2017).

The linkage between atmospheric blocking and precipitation is investigated by many researchers due to the impacts of precipitation on daily activities. Rabinowitz et al. (2018) investigated the relationship between heavy rainfall events associated with atmospheric rivers in the Midwest USA and Pacific Region blocking events during different ENSO phases. They found that 16 heavy rainfall events were observed during the 2000–2015 period, and seven of these events were observed in La Niña (LN) years even though only three LN events occurred during this time. Also, four and five of the 16 events were observed during El Niño (EN) and Neutral (NEU) years, respectively, although there were five and nine EN and NEU years, respectively. There was no statistical relationship between rainfall amounts and blocking characteristics due to the small sample size.

✉ Bahtiyar Efe
efeba@itu.edu.tr

¹ Faculty of Aeronautics and Astronautics, Department of Meteorology, İstanbul Technical University, Maslak, 34469 İstanbul, Turkey

² Atmospheric Sciences Program, University of Missouri, 302 E ABNR Building, Columbia, MO 65202, USA

Rimbu et al. (2015) explored the linkage between summer precipitation extremes and atmospheric blocking events over Romania during the period 1962–2010. The R90p (90th percentile is used as the threshold) index is used to determine extreme rainfall events. Rimbu et al. (2015) determined that blocking events in the sectors (0° – 40° E and 50° – 70° E) are associated with a significant portion of the extreme precipitation variability during summer over Romania.

Sousa et al. (2017a) examined the relationship between blocking locations and European precipitation regimes on both the seasonal and annual time scales. In the regions directly under the influence of blocking, there was a decreased frequency of moderate rainfall events resulting in a reduction of total precipitation. On the other hand, there was an increase in the frequency of extreme rainfall events on the southern flank of blocking events, causing an overall precipitation increase in these regions.

Nunes et al. (2017) investigated the monthly precipitation extremes for two global regions (the central USA and southwest Russia). Nunes et al. (2017) used the meteorological data from Columbia, Missouri during the period of 1889–2014 within the central USA and in Belgorod from 1944 to 2014 for southwest Russia. Monthly departures greater than 3 standard deviations from mean seasonal temperature and the three wettest and driest months for precipitation were used as the criterion to define an extreme event. In the central USA, extreme wet and dry years were associated with NEU years, whereas in southwest Russia, EN and NEU years were responsible for most of the precipitation extremes.

Baltacı et al. (2017) investigated the relationship between teleconnection patterns and Turkish extreme events for the period 1965–2014. Above normal precipitation in the western part of Turkey was linked to the positive phase of Arctic Oscillation (correlation coefficient (CC) around -0.5). In contrast, positive precipitation anomalies were observed over the Black Sea and Aegean regions during the positive phase of the East Atlantic–Western Russia pattern.

The paper of Tayanç et al. (1998) is the first study that mentions blocking as related to a blizzard event, investigating one of the most famous blizzards that occurred in Istanbul, Turkey. This event lasted from 3 to 10 March 1987. The proximate cause of the blizzard was a cyclone that was located in the Balkan region of Europe. The cyclone persisted within the same region for approximately 10 days. Tayanç et al. (1998) determined that the blizzard was associated with an upper-level cyclone, which in turn was associated with blocking.

Atmospheric blocking was observed to be associated with several extreme events in Turkey, including a flash flood event during 7–10 September 2009, during which 31 people died (Kömüscü and Çelik 2013). Also, blocking was associated with a devastating cyclone that caused strong winds (> 80 kts) and fatal incidents, including forest fires during the period of 18–22 April 2012 (Sirdas et al. 2017). One of the wettest winters in the history of Turkey occurred in 1985 (Türkeş and Erlat 2005).

However, blocking was not the focus of these studies which investigated severe weather phenomena.

The scope of this study is to investigate the effects of blocking on the mean annual precipitation frequency for the climate of Turkey. This study is unique regarding three aspects of Turkish climate that will be investigated here. This is the second part of the first climatological study on the impact of blocking that focuses on Turkey only. In the first part, Bahtiyar Efe 2019 (The Relationship Between Atmospheric Blocking and Temperature Anomalies in Turkey between 1977–2016, unpublished) investigated the effects of blocking events on temperature. There are studies that focus on the relationship between blocking activity and climate for the Eurasian region, but these mentioned Turkey only briefly (e.g., Sousa et al., 2017a, b). Studies examining the regional impact of blocking on climate are not unique (e.g., Nunes et al. 2017). Secondly, observational data is used in this study in order to identify the mean precipitation frequency (MPF) in Turkey during blocked days and compares these to nonblocked days. Lastly, this is the first study that investigates the role of blocking on MPF during all seasons for not only our study region but also for the globe.

This paper is organized as follows. The data and methodology are described in Section 2. Then, the annual and seasonal MPF distribution and the relationship between blocking parameters and MPF are presented in Section 3 and the investigation of outstanding blocking events as well as their association with ENSO is presented in Section 3. The results are summarized and discussed in Section 4.

2 Data and methodology

2.1 Data

The dataset used here was the National Centers for Environmental Prediction (NCEP) and National Center for Atmospheric Research (NCAR) Reanalysis-1 dataset (Kalnay et al. 1996), which has 6-h temporal solution and $2.5^{\circ} \times 2.5^{\circ}$ spatial (latitude–longitude) resolution. There are diverse data types available for both the surface and at mandatory pressure levels available from 1948 to present. The daily 500-hPa geopotential height data from NCEP–NCAR Reanalysis-1 for 0000 UTC were used in this study for the period of 1 January 1977 to 31 December 2016. The 500-hPa geopotential height data provided by NCEP–NCAR is preferred by several studies in order to detect blocking (Mokhov et al. 2014; Sitnov et al. 2014; Bahtiyar Efe 2019, unpublished). The study domain was selected as the region bordered by 20° W– 90° E and 30° N– 90° N in order to identify all blocking events that can impact Turkey. A composite map of 10 blocking events with the highest and lowest MPF values is plotted within this domain and examined in Section 3.

The daily total precipitation data for 77 surface stations located in all regions of Turkey were obtained from the Turkish State Meteorological Service. All of these stations have data spanning from 1 January 1977 to 31 December 2016, and thus, the dataset is continuous. The location of the stations is presented in Fig. 1.

2.2 Methodology

The blocking criterion used here is the modified version of blocking detection that was described in TM90, and is used by many studies (e.g., Barriopedro et al. 2006). For this methodology, two height gradients are calculated daily for each longitude as follows:

$$\begin{aligned} \text{GHGS} &= \frac{Z_{\lambda, \varphi_0} - Z_{\lambda, \varphi_S}}{\varphi_0 - \varphi_S} \\ \text{GHGN} &= \frac{Z_{\lambda, \varphi_N} - Z_{\lambda, \varphi_0}}{\varphi_N - \varphi_0} \end{aligned} \tag{1}$$

where

$$\begin{aligned} \varphi_S &= 40^\circ + \Delta \\ \varphi_0 &= 60^\circ + \Delta \\ \varphi_N &= 77.5^\circ + \Delta \\ \Delta &= -5^\circ, -2.5^\circ, 0, 2.5^\circ, 5^\circ \end{aligned} \tag{2}$$

and $Z_{\lambda, \varphi}$ is the geopotential height at longitude λ and latitude φ . The GHGS (geopotential height gradient in the southern part of φ_0) is proportional to the zonal component of the geostrophic wind and GHGN (geopotential height gradient in the northern part of φ_0) is included to exclude nonblocked flows.

This version described in (1) and (2) differs from the original TM90 criterion in that the value of φ_N , numbers of Δ , and values of Δ are based on the $2.5 \times 2.5^\circ$ resolution of the NCEP–NCAR dataset. Any longitude is accepted as blocked when both the GHGS and GNGN indicate the condition expressed by (3) for at least one of the five Δ values:

$$\begin{aligned} \text{GHGS} &> 0 \\ \text{GHGN} &< -10 \text{ geopotential m}^\circ \text{ lat} \\ Z(\lambda, \phi_0) - Z(\lambda, \varphi_0) &> 0 \end{aligned} \tag{3}$$

To verify the minimum longitudinal extent criteria, five (12.5°) or more adjacent grid points are required to satisfy the criteria described in (3) simultaneously, with the allowance of one nonblocked longitude between the blocked longitudes. This condition is consistent with Barriopedro et al. (2006). A 5-day threshold is used in this study for the minimum duration criteria as most authors have used (Treidl et al. 1981; Lupo and Smith 1995; Shabbar et al. 2001; Scherrer et al. 2006). Blocking intensity (BI) is calculated as described in Barriopedro et al. (2006) according to the method defined by Wiedenmann et al. (2002). The blocking center definition and temporal algorithm to track blocking events used in this study are described also in Barriopedro et al. (2006).

The precipitation frequency value is calculated as the ratio between the number of days with precipitation to the total number of days in the defined period. For singular blocking events, it is calculated as the ratio between the days with precipitation to the blocking duration. The relationship between blocking properties (duration, BI, and longitudinal extent) and MPF during blocking events was determined using the Pearson correlation coefficient (Pearson 1896). The significance of the relationship was tested by using the t -distribution

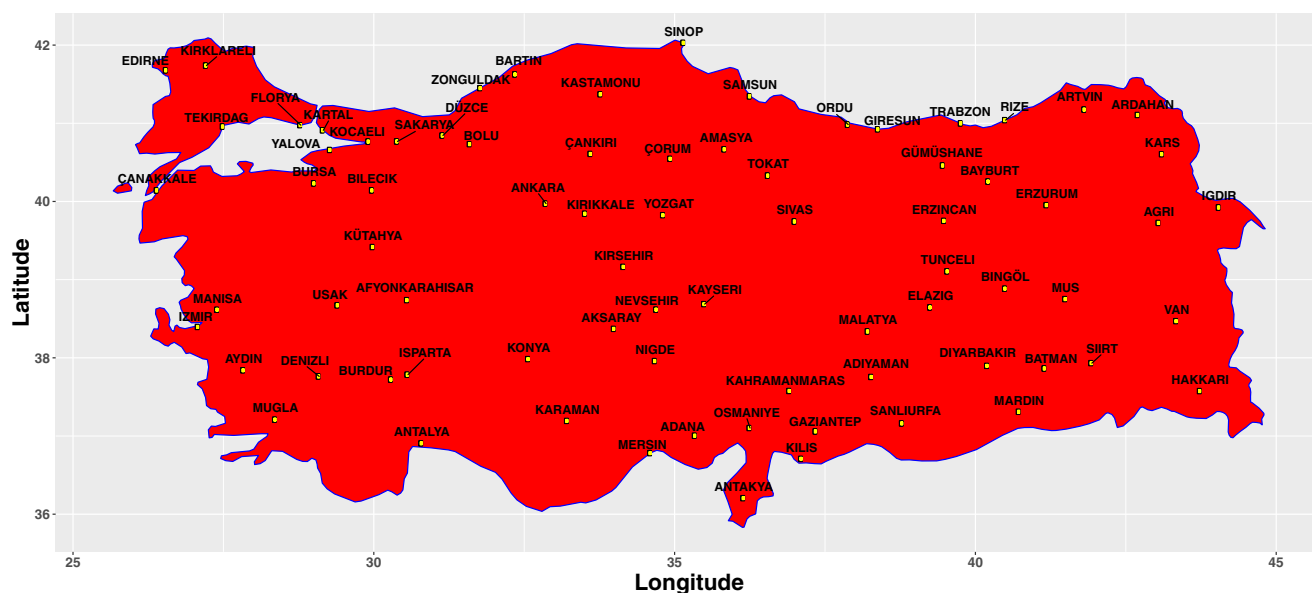


Fig. 1 Location of the stations used in this study

with $N-2$ degrees of freedom. The correlation coefficients were introduced for the entire dataset if it is significant at 95% confidence level or not, and the significance or insignificance was addressed. The MPF during blocked days was stratified by season (December, January, and February for winter; March, April, and May for spring; June, July, and August for summer; and September, October, and November for fall). All figures except the 500-hPa composite maps and 850-hPa specific humidity maps for important events are illustrated via the ggplot2 R-package (Wickham 2016). All calculations are performed using R-programming (R Core Team 2018; Wickham et al. 2018). The 500-hPa composite maps were plotted using the NCEP–NCAR website, and the 850-hPa charts were plotted using the University of Plymouth website.

The data are classified also by the ENSO phase. The distribution of ENSO phases is shown in Table 1 and more information about the ENSO definition used here can be found in Bove et al. (1998). Only the statistically significant correlation coefficient values at 95% significance level were presented for ENSO phases.

3 Results

3.1 Annual MPF distribution

The MPF across Turkey during blocked days (nonblocked days) is shown in Fig. 2 (Fig. 3). The MPF across Turkey for the study period during blocked days (during nonblocking days) varies between 0.15 and 0.43 (0.12 and 0.38). The highest precipitation frequencies were observed along the Black Sea coastline and the northeastern part of the Marmara Region during both blocked and nonblocked events. The lowest MPF values were observed in southern Turkey, especially along the Mediterranean coastline and several cities in South Anatolia Region during blocked and nonblocked days. Rize, Giresun, and Ordu are the cities that have the highest precipitation frequencies with values of 0.43, 0.39,

and 0.36 during blocked days and 0.38, 0.32, and 0.29 during nonblocked days, respectively. Mersin, Karaman, and Osmaniye (Osmaniye, Mersin, and Karaman) are the cities that have the lowest precipitation frequencies with values of 0.15, 0.16, and 0.16 during blocked days (0.12, 0.13, and 0.13 during nonblocked days), respectively.

The ratio of precipitation frequency during blocked days with respect to nonblocked days is shown in Fig. 4. Blocking events increase the MPF across the entire country. This increase in precipitation frequency ranges from 12 to 42% across Turkey. The inner part of Anatolia observed the higher ratio of precipitation frequency values, whereas the western Black Sea Region was associated with the lowest values. Konya, Kırklareli, and Çanakkale are the stations that have the highest precipitation frequency change with values of 48, 42, and 41%, respectively. Rize, Artvin, and Giresun have lowest precipitation frequency change with values of 13, 14, and 18%, respectively. Thus, overall, blocking has an enhancing effect on the MPF across Turkey.

3.2 Seasonal MPF distributions

MPF during blocked days (nonblocked days) in all seasons is shown in Fig. 5 (Fig. 6). During blocked (nonblocked) days, the winter season has the highest precipitation frequency across the country with an average value of 0.31 (0.26). During blocked (nonblocked) days, the stations have precipitation frequency values in the range of 0.15 and 0.54 (0.10 and 0.40). For blocked (nonblocked) days, the inner part of Marmara Region, the coastal parts of the Black Sea Region, and the southwest part of East Anatolia Region (the west part of the Marmara Region, the Black Sea coastline, and the southwest part of East Anatolia Region) have higher precipitation frequency values. During blocked (nonblocked) days, Zonguldak, Rize, and Kocaeli (Zonguldak, Bartın, and Rize) have the highest precipitation frequencies with values of 0.54, 0.48, and 0.48 (0.40, 0.39, and 0.39), respectively. During blocked (nonblocked) days, the vast majority of the inner part of the Aegean Region, Central Anatolia Region, and Mediterranean Region (Central Anatolia Region, northeast part of East Anatolia Region, and the inner part of the Aegean Region) have lower values. For blocked (nonblocked) days, Iğdır, Osmaniye, and Erzincan (Iğdır, Ardahan, and Erzurum) have the lowest precipitation frequency with values of 0.15, 0.19, and 0.21 (0.10, 0.16, and 0.16), respectively.

During blocked (nonblocked) days, the spring season observed an MPF of 0.29 (0.24) across Turkey, with a minimum value of 0.13 (0.14) and maximum of 0.41 (0.36). For blocked (nonblocked) days, a large portion of the East Anatolian Region and Black Sea Region (East Anatolia Region and east part of the Black Sea Region) have greater values. During blocked (nonblocked) days, Rize, Giresun, and Muş (Rize,

Table 1 List of ENSO years 1976–2016 (ENSO year begins 1 October of the given year and ends on 30 September of the next year)

	El Niño	Neutral	La Niña
1976	1977–1981	1975	
1982	1983–1985	1988	
1986–1987	1989–1990	1998–1999	
1991	1992–1996	2007	
1997	2000–2001	2010	
2002	2003–2005		
2006	2008		
2009	2011–2013		
2014–2015	2016		

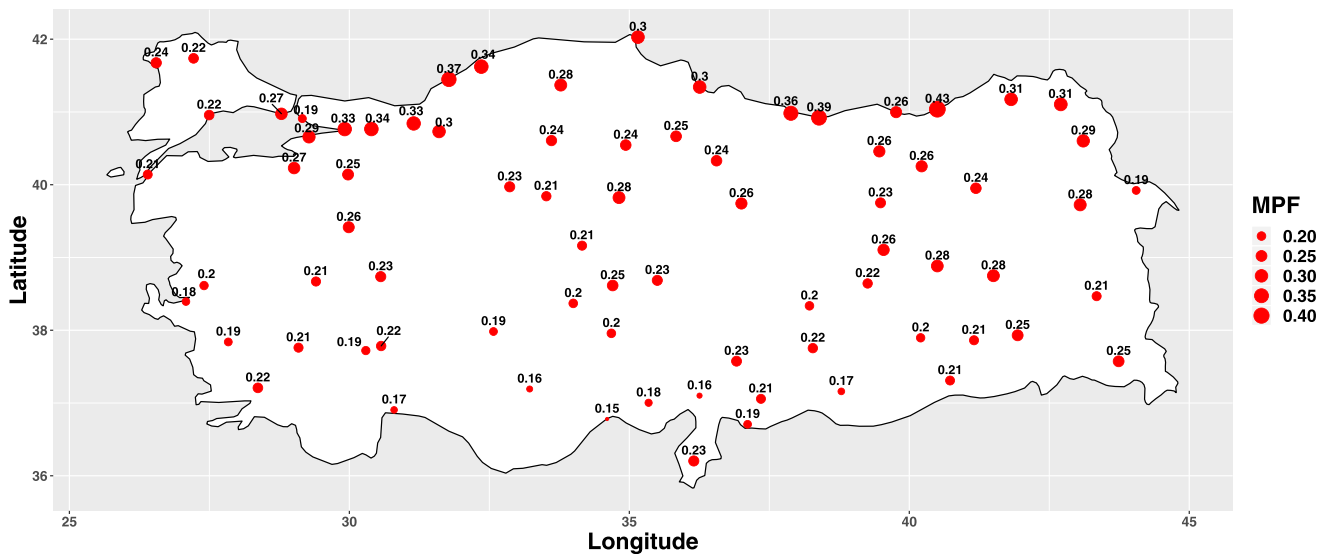


Fig. 2 MPF distribution during blocked days

Giresun, and Ağrı) have the highest precipitation frequencies with values of 0.41, 0.40, and 0.40 (0.36, 0.35, and 0.35), respectively. For blocked (nonblocked) days, the coastal region of the Aegean and Mediterranean Regions and west of the South East Anatolia Regions (the European part of the Marmara Region, the coastline of the Aegean Sea, and the Mediterranean Sea) have lower values of MPF. For blocked (nonblocked) days, Mersin, Antalya, and Kartal (Mersin, Kartal, and Antalya) are the stations with the lowest values of 0.14, 0.17, and 0.18 (0.13, 0.14, and 0.14), respectively.

Summer is the driest season across Turkey and precipitation frequency decreases sharply even on blocked days. During blocked (nonblocked) days, MPF ranges between a value of 0.02 (0.01) and a maximum value of 0.38 (0.36) with the mean of 0.13 (0.09). For blocked (nonblocked) days, the cities in the northern part of the country particularly along the

Black Sea coastline (the Black Sea coastline, the northern part of East Anatolia Region, and east of Marmara Region) have higher MPF. For blocked (nonblocked) days, Rize, Ardahan, and Kars (Rize, Kars, and Ardahan) have the highest MPF with values of 0.38, 0.37, and 0.30 (0.36, 0.31, and 0.27), respectively. During blocked (nonblocked) days, the Southeast Anatolia Region, south of East Anatolia Region, coastline of the Mediterranean, and the Aegean Sea (the southeast Anatolia Region, the southern part of East Anatolia Region, and the coastline of both the Aegean and the Mediterranean Sea) have lower MPF. For blocked (nonblocked) days, Şanlıurfa, Diyarbakır, and Antalya (Kilis, Şanlıurfa, and Mardin) have the lowest MPF values of 0.02, 0.02, and 0.03 (0.01, 0.01, and 0.01), respectively.

Lastly, during fall season blocked (nonblocked) days, MPF fluctuates between 0.12 and 0.45 (0.1 and 0.4) with

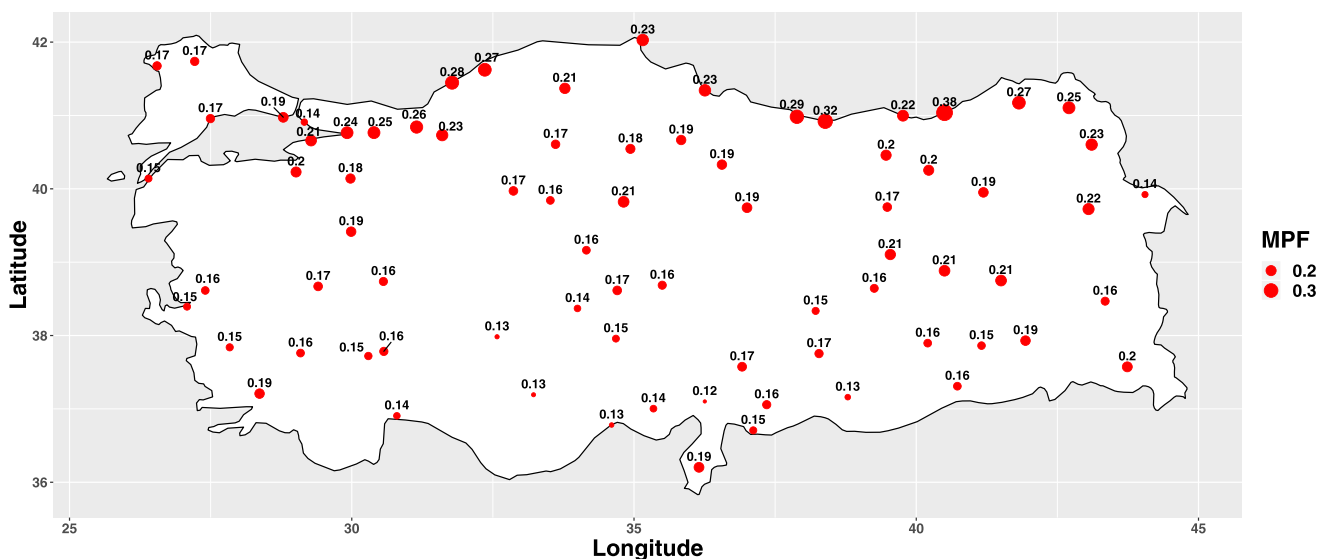


Fig. 3 As in Fig. 2, except for nonblocked days

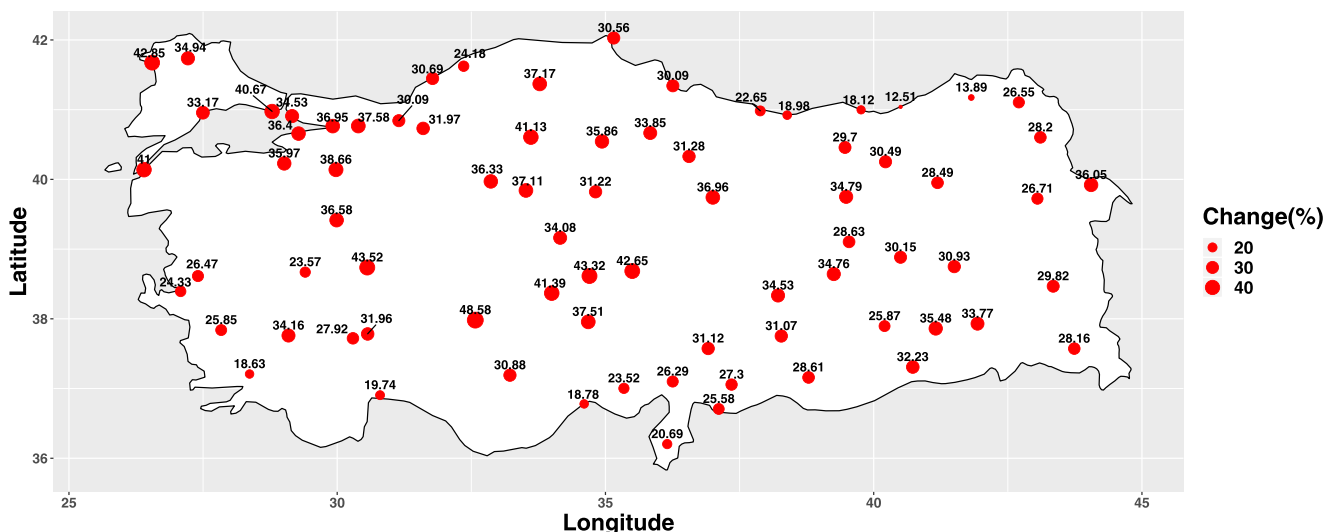


Fig. 4 Change in MPF (%) during blocked days with respect to nonblocked days

the national average at 0.21 (0.16). During blocked (nonblocked) days, the coastal region of the Black Sea Region and the eastern part of the Marmara Region (the northern regions) have higher values. For blocked (nonblocked) days, Rize, Ordu, and Zonguldak (Rize, Giresun, and Ordu) have the highest MPF with values of 0.45, 0.39, and 0.38 (0.40, 0.35, and 0.32), respectively. During blocked (nonblocked) days, the Southeast Anatolia Region and Mediterranean Region (the southern regions) have lower values of MPF. For both blocked and nonblocked days, Şanlıurfa, Karaman, and Mardin have the lowest MPF values of 0.12, 0.12, and 0.13 and 0.10, 0.10, and 0.10, respectively.

In addition, the change of MPF during blocked days with respect to nonblocked days is investigated (Fig. 7). The change of MPF in blocked days during all seasons is positive. Thus, we can conclude that blocking causes an increase in the frequency of rainy days. In winter, the average change in MPF is 19%, with a minimum value of 1% and a maximum of 50%. The higher changes occurred in the northeast part of the country (37% and higher), the southern part of Central Anatolia Region (28% and higher), and eastern part of the Marmara Region (31% and higher). Iğdır, Florya, and Ardahan observed the greatest changes with values of 50, 39, and 38%, respectively. The Aegean coastline (7% and lower), Mediterranean coastline (8% and

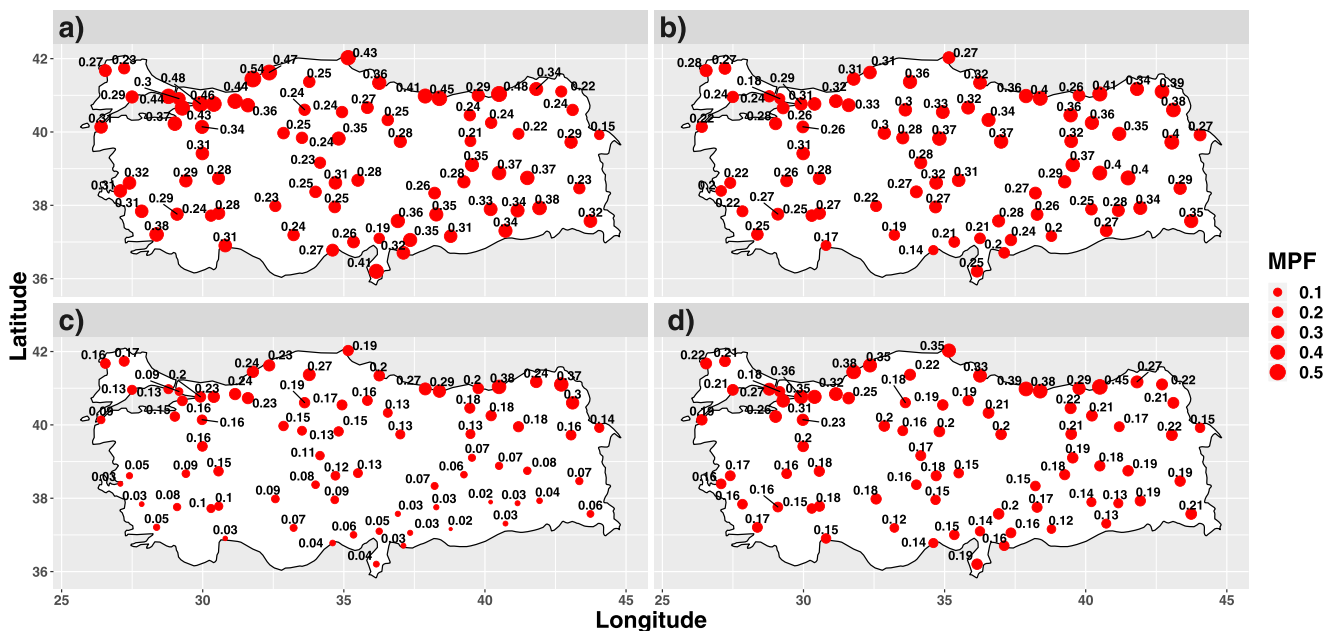


Fig. 5 MPF distribution during blocked days stratified by season

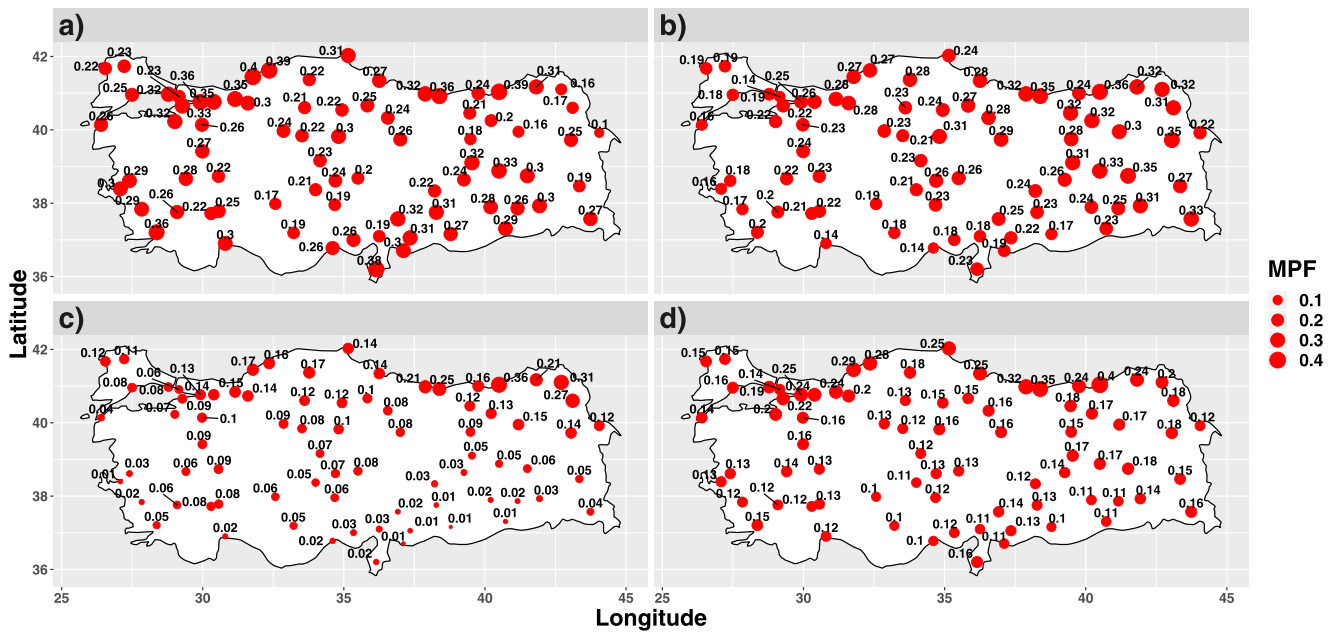


Fig. 6 As in Fig. 5, except for nonblocked days

lower), some cities in the northern part of the Central Anatolia Region (8% and lower), and the vast majority of Southeast Anatolia Region (18% and lower) observed lower changes. Kırklareli (1%), Adana (2%), and Osmaniye (2%) are the cities that observed the lowest changes.

During the spring season, the minimum, mean, and maximum of changes are 4, 19, and 48%, respectively. The Thracian part of the Marmara Region and several cities in the northern part of the Central Anatolia Region observed greater changes (higher than 33 and 27%, respectively). Edirne, Kırklareli, and Çanakkale are all located in the Thracian part of the Marmara Region and observed the

highest changes (48, 41, and 40%, respectively). The southern part of the East Anatolia Region, the South East Anatolia Region, and the eastern part of the Mediterranean Region observed the lower changes (lower than 10, 16, and 13%, respectively). Artvin, Kilis, and Trabzon observed the lowest change values at 5, 6, and 6%, respectively.

During the summer season, the change in MPF on the stations fluctuated between 4 and 216% with a mean of 60%. This greater value of change in the summer is due to lower MPF during nonblocked days and blocked days. For example, the Kilis station has an MPF of approximately 0.01 during nonblocked days and 0.03 during blocked days; thus, the

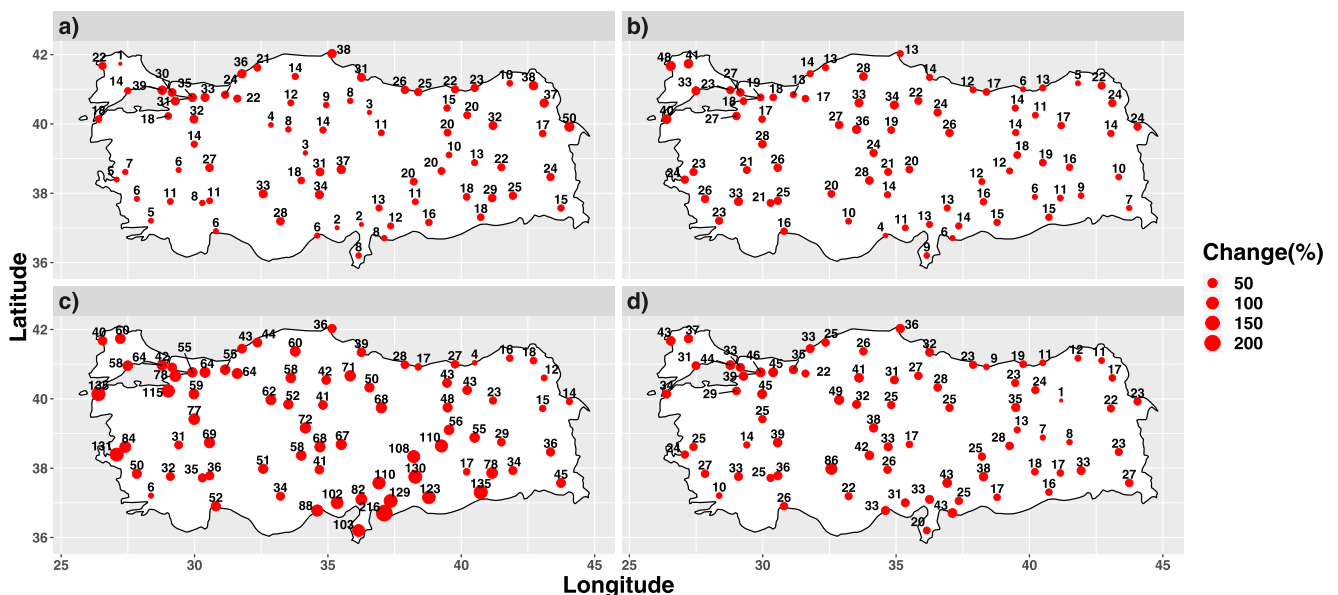


Fig. 7 As in Fig. 4, except as stratified by season

change is 216%. The southern part of the East Anatolia Region and the eastern part of the Mediterranean Region have higher changes (78 and 82% or higher, respectively). Kilis, Çanakkale, and Mardin observed the greatest changes with 216, 135, and 135%, respectively. The northeast part of the country observed lower changes (23% and lower). Rize, Muğla, and Kars observed the lowest changes (4, 6, and 12%, respectively).

During the fall season, the mean MPF changes were 28% nationwide with a minimum of 1% and a maximum of 86%. The northeast part of the Central Anatolia Region, the Marmara Region, and the cities in the neighborhood of the Mediterranean and the South East Anatolia Region have higher changes (32, 37, and 31% or higher, respectively). Konya, Ankara, and Kocaeli have the greatest changes with 86, 49, and 46%, respectively. The eastern part of East Anatolia Region and the eastern Black Sea coastline have smaller changes (23% or lower for both regions). Erzurum, Bingöl, and Muş have the lowest changes (1, 7, and 8%, respectively).

3.3 The relationship between blocking parameters and MPF

3.3.1 Block center location

In this subsection, the relationship between blocking center and MPF is investigated. The study domain is divided into four sectors: 20 W–0, 0–30 E, 30 E–60 E, and 60 E–90 E, respectively. The first sector does not have the same width as the others; however, these are the same domains used by Bahtiyar Efe 2019, unpublished. Also, sectors 2, 3, and 4 are consistent with those defined in Sousa et al. (2017a, b). The MPF ranges between 0.15 and 0.38 with an average of 0.25

when the block center is located in the first sector of the study region (Fig. 8). The Black Sea coastline observes greater values, while the southern part of the Central Anatolia Region and the Mediterranean Region observe lower values. Rize (0.38), Zonguldak (0.35), and Giresun (0.31) have the highest values when the blocking center is located in the first sector. On the other hand, Mersin (0.15), Konya (0.17), and Iğdır (0.17) have the lowest values.

When the block center is located in the second sector, the minimum, mean, and maximum MPF values are 0.17, 0.27, and 0.51, respectively. The Black Sea coastline and the northeastern part of the country have greater values, while the Mediterranean Region, South East Anatolia Region, and Aegean Sea coastline have lower values. Rize, Giresun, and Ordu are the cities with the greatest MPF values (0.52, 0.47, and 0.45, respectively). Mersin, Şanlıurfa, and İzmir have the lowest MPF with the value of 0.17.

For the third sector, the MPF values vary between 0.13 and 0.36 with a mean value of 0.22. Generally, the MPF values are related to the latitudinal position of the stations when the blocking center is located in the third sector. The northern stations, for example, Rize, Giresun, and Zonguldak, have the greatest values, 0.36, 0.34, and 0.31, respectively. The southern stations, for example, Osmaniye (0.13), Şanlıurfa (0.15), and Mardin (0.15), are the stations with the lowest values.

Lastly, for the fourth sector, nationwide, the minimum, mean, and maximum MPF values are 0.10, 0.21, and 0.38, respectively. The eastern part of the Marmara Region and the western part of the Black Sea Region observe the highest values. The Mediterranean Region and the South Anatolia Region observe the lowest values. Zonguldak (0.38), Rize (0.36), and Bartın (0.36) have the greatest MPF values, while

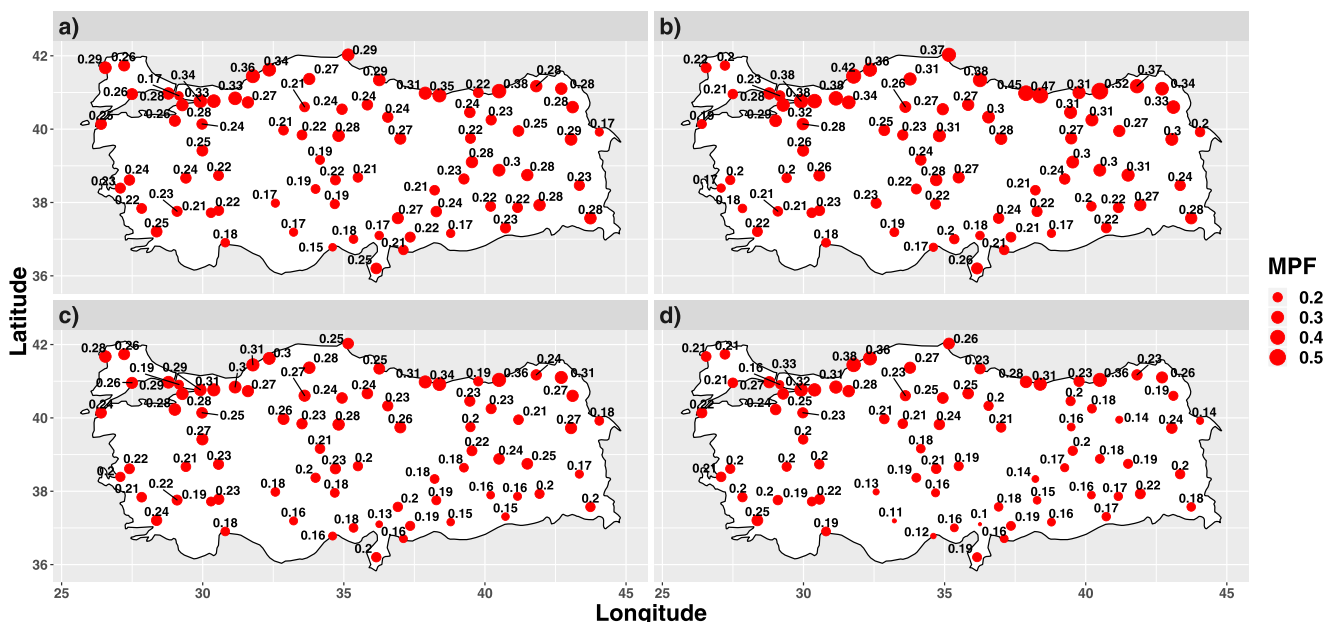


Fig. 8 MPF distribution with respect to the blocking center longitude for a 20° W–0° E, b 0° E–30° E, c 30° E–60° E, and d 60° E–90° E

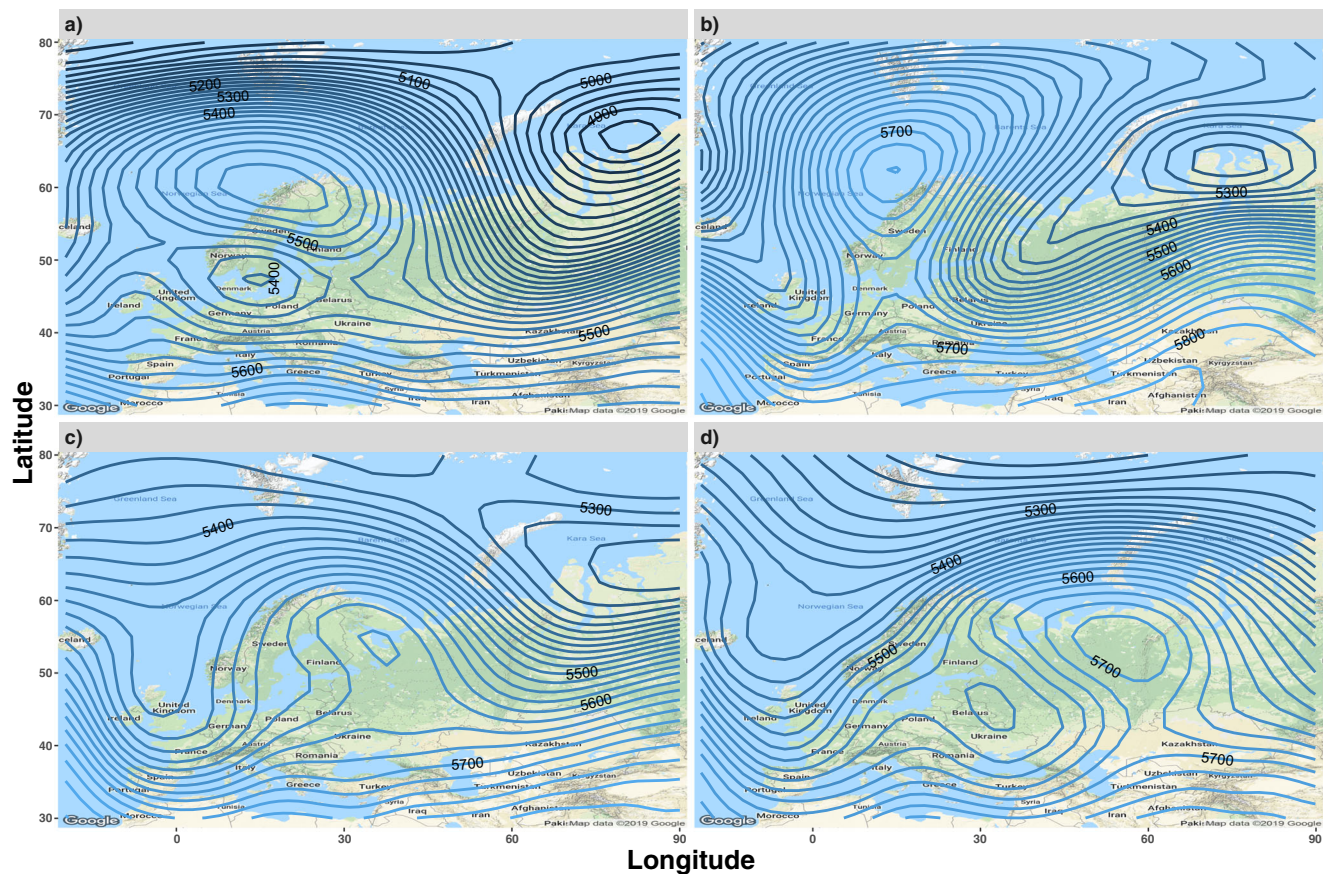


Fig. 9 The 500-hPa height (m) field showing sample blocking events with the blocking center located in the **a** first sector, **b** second sector, **c** third sector, and **d** fourth sector. The height contour interval is 60 m

Osmaniye (0.1), Karaman (0.11), and Mersin (0.12) have the lowest values.

Examples of blocking events that are located in different sectors are shown in the 500-hPa height field (Fig. 9). These events are also the most intense (BI) events observed within those sectors. The representative blocking event located in the first sector is a Rex-type event. Turkey is under the influence of the flow associated with the cyclone located over southeast Europe. The height gradient around the blocking high is relatively weak. The flow is westerly over the entire country, transporting more humid air from the Aegean and Mediterranean Sea into Turkey. The blocking event located in the second sector is an omega-type event. Turkey is located on the downstream flank of the blocking high. There is dry air transport from Europe into the northern part of the country and humid air transport from the Mediterranean into the southern part. The geopotential height gradient is the strongest compared to the other three events indicating stronger flow. The blocking event located in the third sector is also an omega-type event. It has the weakest geopotential height gradient over Turkey and the flow is nearly zonal. The fourth example is also an omega-type blocking event. Turkey is located on the upstream flank of the blocking high. The geopotential height

gradient is weak over the northern part of the country but stronger over the southern part.

3.3.2 Blocking duration vs. MPF

The relationship between blocking duration and MPF stratified by ENSO phase is shown in Fig. 10. As mentioned in Section 2, the correlation coefficient for the entire dataset will be given if it is significant at 95% significance level for the next three subsections. However, correlation coefficients statistically significant at the 95% level will be given for ENSO phases. There is no statistically significant relationship observed between blocking duration and MPF in all seasons and for all ENSO phases except NEU for spring. The correlation coefficient of the entire dataset for winter, spring, summer, and fall is -0.01 (not statistically significant (NSS)), 0.1 (NSS), 0.03 (NSS), and 0.02 (NSS), respectively. Only, NEU was statistically significant at 95% relationship ($CC = 0.22$) in the spring.

3.3.3 Blocking intensity vs. MPF

The relationship between BI and MPF is shown in Fig. 11. During winter, the CC between BI and MPF is 0.18 and is

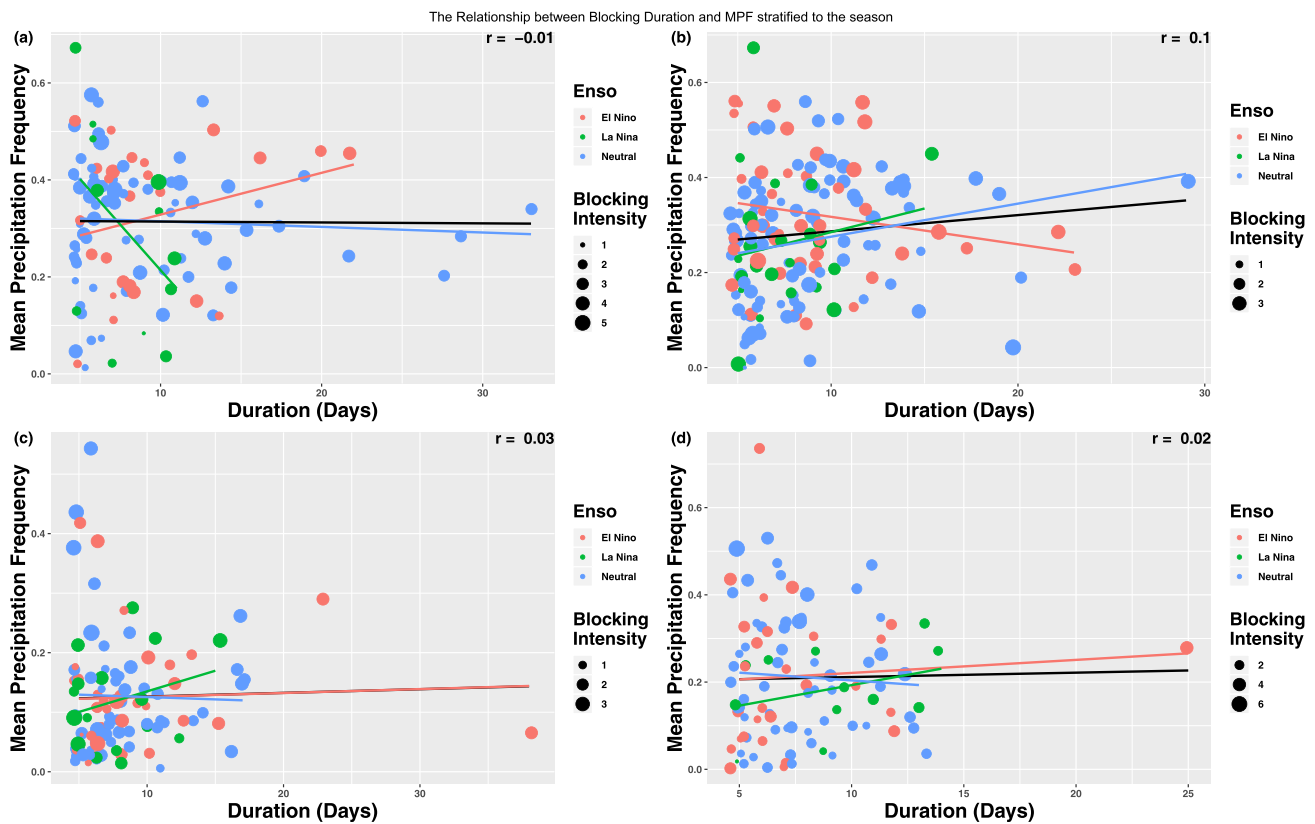


Fig. 10 The relationship between blocking duration and MPF stratified by season, for **a** winter, **b** spring, **c** summer, and **d** fall

NSS. In spring, the CC is 0.1 and is NSS for the entire dataset. During summer, the entire dataset has a positive relationship (CC = 0.35, statistically significant at a 95% level). NEU years have also a positive relationship significant at the 95% level (CC = 0.50). Lastly, during the fall season, the whole data was statistically significant at the 95% confidence level indicating a positive relationship (CC = 0.43). The NEU years have a positive relationship with CC value of 0.48, significant at the 95% confidence level.

3.3.4 Blocking longitudinal extent vs. MPF

The relationship between the longitudinal extent of blocking and MPF is stratified by the ENSO phase and shown in Fig. 12. There is a positive relationship (CC = 0.15, NSS) during winter for the entire dataset. In spring, there is a positive relationship (CC = 0.26, statistically significant at the 95% level) for the entire dataset. The NEU years also have a statistically significant relationship (CC = 0.37, statistically significant at the 95% level). During summer, the CC is 0.29 (significant at the 95% level). The EN years have a CC of 0.32, significant at the 95% level. Lastly, fall has a CC of 0.25 (significant at the 95% level). Also, the NEU years have positive relationships (CC = 0.33, significant at the 95% level.).

3.4 The 500-hPa conditions and ENSO phases for the 10 lowest/highest MPF

The average 500-hPa geopotential height conditions during the 10 blocking events that have the lowest and the highest MPF values stratified by season are shown in Fig. 13. The dates for these events are shown in Table 2. The block center is located near 15° E and 60° N during the winter season for those events with higher MPF. The mean BI during these events is 2.81. According to the 850-hPa charts, there was considerable water vapor advection from the Mediterranean Sea during the events that have the greatest MPF. The representative 850-hPa maps are shown in Fig. 14. The mean BI for the events with the lowest MPF values during winter is 1.87, and the mean center position is located close to 20° E and 60° N. Here, the water vapor transport is from a different direction. In the representative 850-hPa map, the specific humidity is transported from the Balkans to Turkey (Fig. 14).

During the spring season, the highest MPF blocking events have a mean block center position near 20° E and 60° N. The mean BI is 2.23 during these events. According to the 850-hPa charts, there was considerable water vapor advection from the Mediterranean Sea during the events that have the greatest MPF (Fig. 14). The BI during the lowest blocking events is 2.25 with the center location near 23° E and 55° N. In the representative 850-hPa chart, the air masses are transported

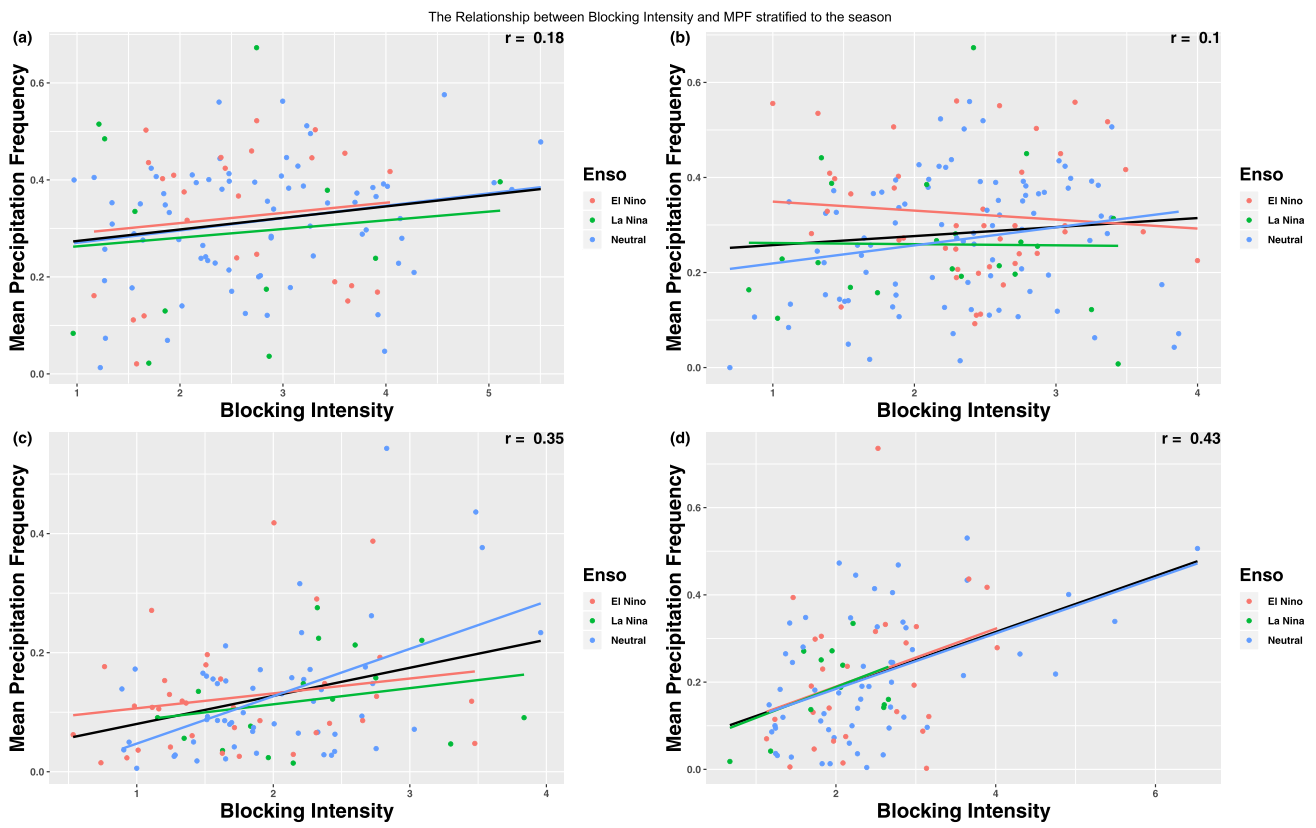


Fig. 11 As in Fig. 10, except for BI

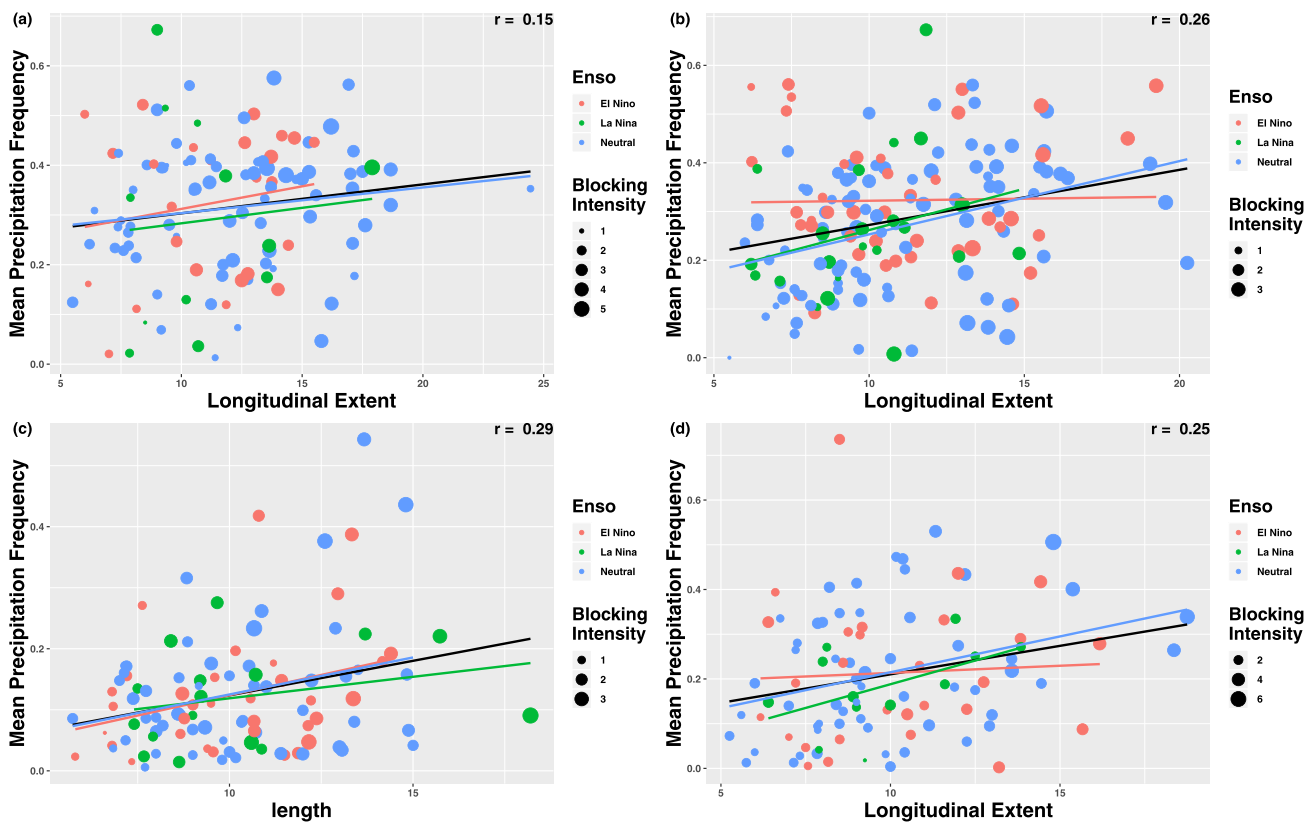


Fig. 12 As in Fig. 10, except for blocking longitudinal extent

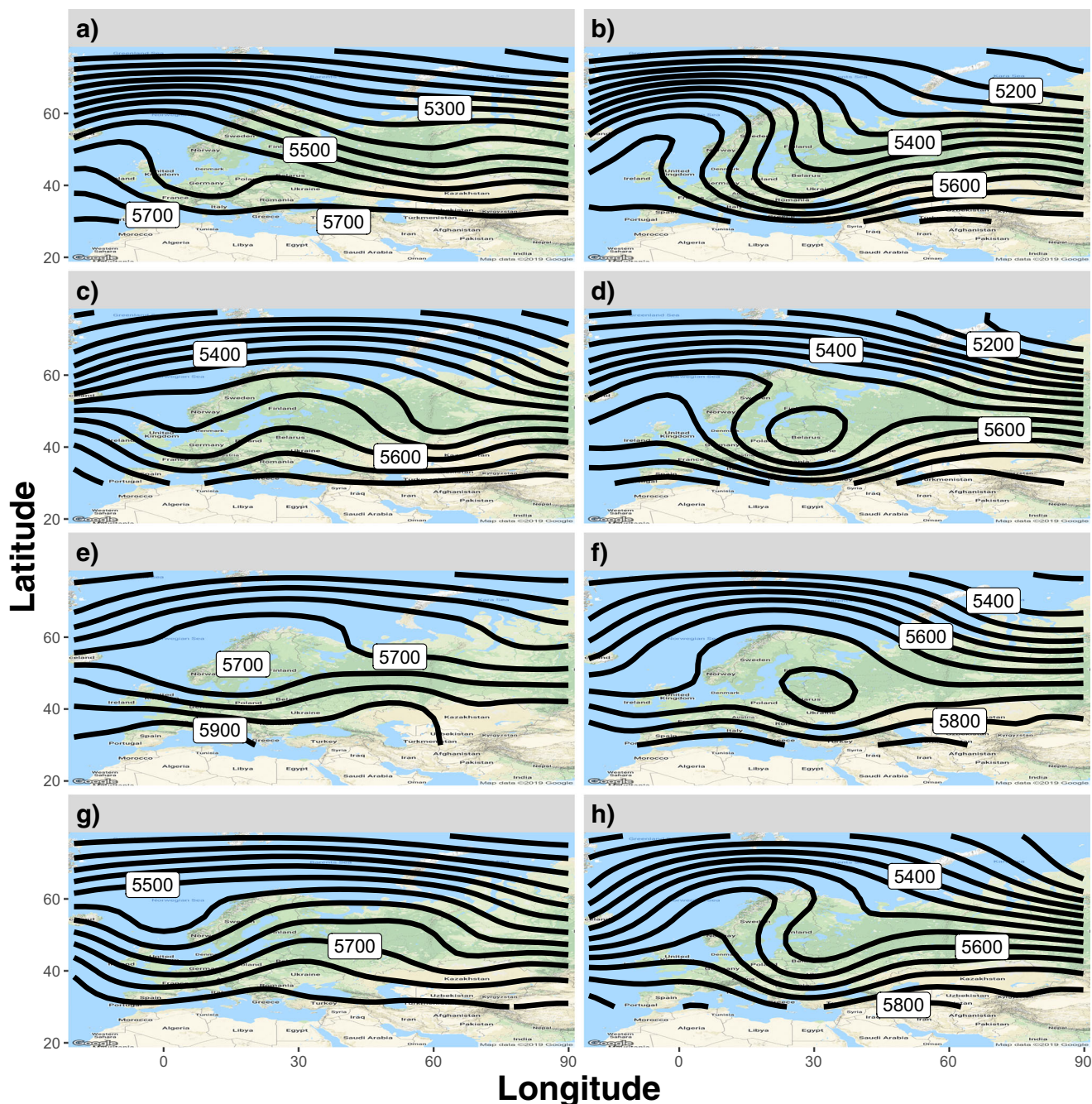


Fig. 13 The composite map of 500 hPa geopotential height data (m) of the 10 wettest (highest MPF) and driest (lowest MPF) events for **a, b** winter; **c, d** spring; **e, f** summer; and **g, h** fall season

from locales that have similar specific humidity to Turkey for the driest blocking events (Fig. 14).

During the summer season, the highest events have a mean BI value of 2.34 and the blocking center is located near 35° E and 65° N. According to the 850-hPa charts, there was considerable water vapor advection from the Mediterranean Sea during the events that have the greatest MPF (Fig. 14). A jet stream was observed where there were strong pressure gradients over the Mediterranean area (not shown). The mean BI during blocking events with the lowest MPF is 1.65 and the blocking center is

located approximately at 35° E and 65° N similar to that of the highest MPF blocking events for this summer. There is weak water vapor advection during dry events or water vapor transport from Turkey. In the representative 850-hPa chart, weak specific humidity advection occurred over the western and northern parts of the nation, while specific humidity transport into Turkey occurred over southeast of the country (Fig. 14).

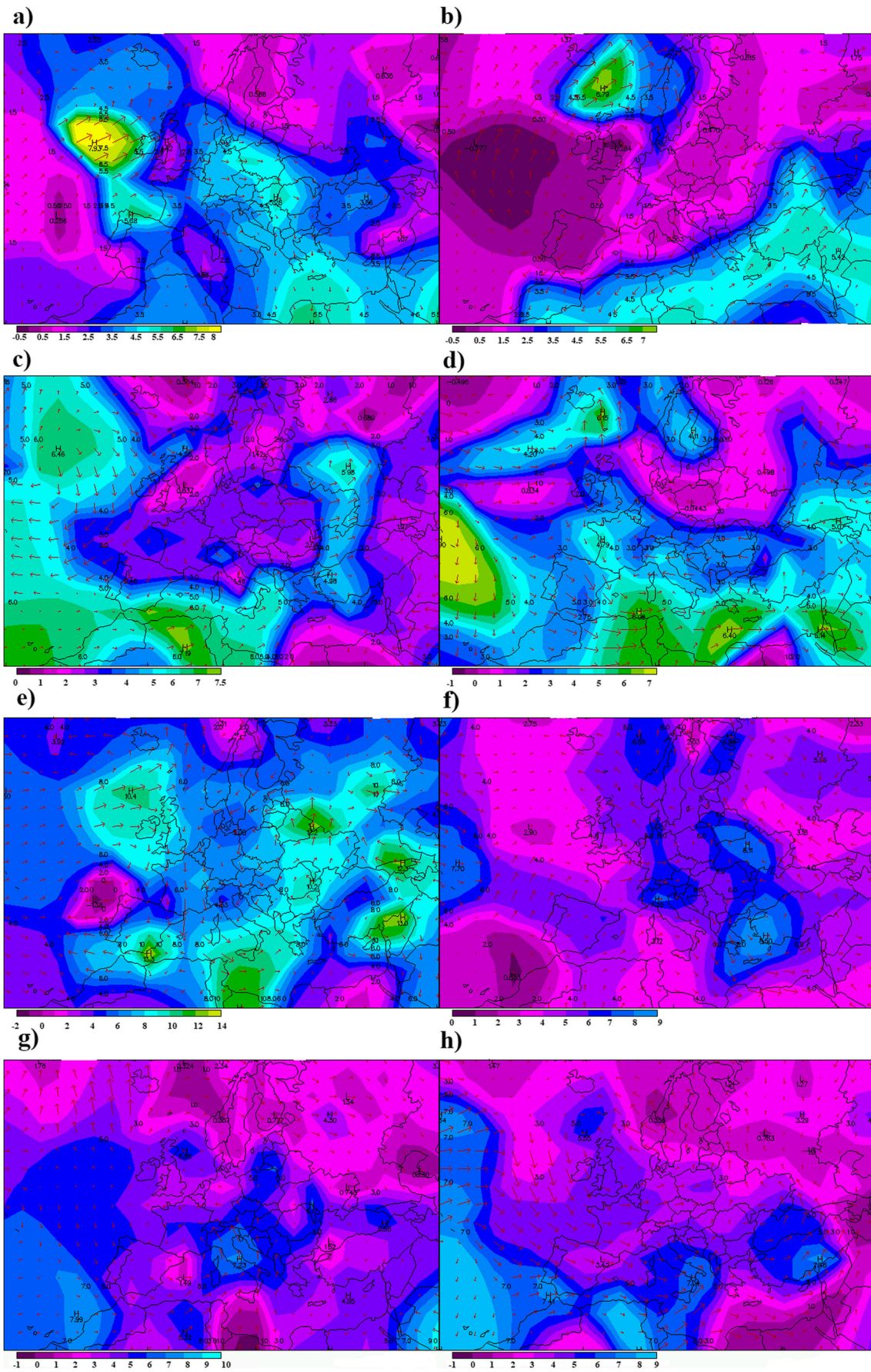
For the fall season, an omega-shaped blocking event is observed in the average 500-hPa geopotential height map. The mean BI is 2.81 and the blocking center is located close

Table 2 The dates for the 10 wettest and driest blocking events

Season	No.	Dry		Wet	
		Start	End	Start	End
Winter	1	1984 February 23	1984 February 27	1991 December 01	1991 December 13
Winter	2	1984 December 01	1984 December 05	1994 December 01	1994 December 05
Winter	3	1987 January 11	1987 January 24	1998 December 08	1998 December 12
Winter	4	1989 January 24	1989 February 01	2001 November 30	2001 December 04
Winter	5	1992 January 11	1992 January 17	2001 December 07	2001 December 19
Winter	6	1998 January 16	1998 January 20	2002 January 04	2002 January 09
Winter	7	2005 December 10	2005 December 15	2009 February 19	2009 February 24
Winter	8	2006 February 21	2006 February 26	2009 December 12	2009 December 18
Winter	9	2008 January 18	2008 January 24	2011 January 27	2011 February 01
Winter	10	2011 January 15	2011 January 23	2014 December 29	2015 January 02
Spring	1	1980 May 31	1980 June 04	1977 March 16	1977 March 20
Spring	2	1985 March 03	1985 March 13	1987 March 06	1987 March 16
Spring	3	1986 March 09	1986 March 17	1987 April 12	1987 April 16
Spring	4	1986 March 19	1986 March 28	1988 April 17	1988 April 21
Spring	5	1986 April 23	1986 April 28	1996 February 29	1996 March 05
Spring	6	1989 April 02	1989 April 06	1998 May 13	1998 May 19
Spring	7	1993 February 25	1993 March 01	1999 March 29	1999 April 03
Spring	8	1994 April 14	1994 April 18	2001 May 04	2001 May 12
Spring	9	1997 March 08	1997 March 13	2002 March 23	2002 March 31
Spring	10	2004 April 09	2004 April 13	2002 April 03	2002 April 10
Summer	1	1977 July 06	1977 July 11	1979 June 01	1979 June 05
Summer	2	1987 July 13	1987 July 17	1982 June 01	1982 June 05
Summer	3	1987 July 19	1987 July 23	1984 May 31	1984 June 04
Summer	4	1991 July 28	1991 August 03	1988 June 16	1988 June 21
Summer	5	1995 July 29	1995 August 03	1992 June 01	1992 June 21
Summer	6	2000 July 12	2000 July 19	1995 May 31	1995 June 04
Summer	7	2004 July 20	2004 July 24	1997 June 07	1997 June 12
Summer	8	2005 July 09	2005 July 13	2010 June 23	2010 June 27
Summer	9	2006 August 04	2006 August 14	2011 May 31	2011 June 04
Summer	10	2008 July 19	2008 July 24	2014 June 02	2014 June 07
Fall	1	1981 August 28	1981 September 02	1979 October 24	1979 October 25
Fall	2	1986 November 17	1986 November 23	1985 October 14	1985 October 19
Fall	3	1988 September 14	1988 September 20	1989 November 09	1989 November 19
Fall	4	1994 September 18	1994 September 22	1993 November 10	1993 November 16
Fall	5	2000 November 06	2000 November 11	1996 October 23	1996 October 28
Fall	6	2001 September 14	2001 September 22	1997 November 17	1997 November 23
Fall	7	2008 November 01	2008 November 07	1998 November 29	1998 December 05
Fall	8	2010 November 18	2010 November 22	2005 October 15	2005 October 19
Fall	9	2013 September 06	2013 September 11	2006 October 13	2006 October 17
Fall	10	2016 November 20	2016 November 24	2009 October 31	2009 November 05

to 20° E and 65° N. According to the 850-hPa charts, there was considerable water vapor advection from the Mediterranean Sea region during the events that have the greatest MPF (Fig. 14). For the lowest MPF blocking events, the BI and blocking center are 1.87 and 35° E and 60° N,

respectively. There is weak water vapor advection during dry events, or there was water vapor transport out of the region of Turkey. In the representative 850-hPa chart, weak specific humidity advection occurred over the western part of the



◀ **Fig. 14** The representative 850 hPa charts for **a** dry winter, **b** wet winter, **c** dry spring, **d** wet spring, **e** dry summer, **f** wet summer, **g** dry fall, and **h** wet fall

region, while specific humidity divergence occurred over the east part of the country (Fig. 14).

The ENSO phases during the 10 blocking events that have highest MPF values stratified by season are shown in Table 3. During the winter season, five of the 10 highest MPF blocking events occurred in NEU years, while three (two) of them took place in EN (LN) years. There is a slight tendency toward LN (away from NEU) events since these years comprised only 12% (62.5%) of the years in the study period although 20% (50%) of the events were observed in LN (NEU) years. In the spring season, five of 10 events were observed during EN years, while four (one) were during NEU (LN) years. During this season, EN years are dominant as 50% of the events were observed in these years. For the summer season, six of 10 events were NEU season events and four of 10 occurred during EN years. No events were observed during LN years. Thus, there is a greater tendency for an occurrence during EN events in this season. During the fall season, six of 10 events were NEU events, while three (one) of them were EN (LN) events. This distribution would be expected as the occurrence of high MPF events was random.

3.5 Analysis of the blocking case with the greatest MPF

The average 500-hPa height for the blocking event that has the greatest MPF is shown in Fig. 15. The blocking event within the study area occurred between 31 October 2009 and 05 November 2009. The omega-shaped blocking event was centered at approximately 30° E and 65° N. The upper-level downstream trough impacted Turkey during this blocking event, and there was moist air advection from southern Europe, across the lifetime of this blocking event. The event was associated with BI, duration, and longitudinal extent with values of 2.52, 6 days, and 20°, respectively. The nationwide MPF was 0.73 and the mean total precipitation was 63.4 mm during this blocking event even though the duration was only 6 days. During this blocking event, heavy rainfall and flash flood events were observed in the Marmara Region (Gazete Vatan 2009), Şanlıurfa (a city in South Anatolia Region, Takvim 2009), and Trabzon (NTV 2009).

4 Summary and discussion

During blocked days, the highest MPF values in Turkey were observed in general along the Black Sea coastline and the northeastern part of the Marmara Region. The lowest MPF values were observed within southern Turkey especially along

Table 3 The ENSO phase for the 10 highest MPF blocking events stratified by season

Start date	Winter			Spring			Summer			Fall				
	ENSO	Mean prep freq.	Start date	ENSO	Mean prep freq.	Start date	ENSO	Mean prep freq.	Start date	ENSO	Mean prep freq.	Start date	ENSO	Mean prep freq.
1998 December 08	LN	0.66	1999 March 29	LN	0.66	2014 June 02	NEU	0.52	2009 October 31	EN	0.73	2009 October 31	EN	0.73
2002 January 04	NEU	0.57	1996 February 29	NEU	0.56	1979 May 13	NEU	0.42	1998 November 29	LN	0.67	1998 November 29	LN	0.67
2001 November 27	NEU	0.55	1977 March 16	EN	0.55	2010 June 23	EN	0.4	1996 October 23	NEU	0.52	1996 October 23	NEU	0.52
2001 December 07	NEU	0.55	1987 March 06	EN	0.54	1988 June 16	EN	0.38	1979 October 24	NEU	0.49	1979 October 24	NEU	0.49
2014 December 29	EN	0.52	1988 April 17	EN	0.54	1982 May 30	NEU	0.37	1985 October 14	NEU	0.46	1985 October 14	NEU	0.46
2011 January 27	LN	0.5	1998 May 13	EN	0.54	1997 June 07	NEU	0.3	1989 November 09	NEU	0.45	1989 November 09	NEU	0.45
1994 December 01	NEU	0.5	2001 May 04	NEU	0.54	1992 May 15	EN	0.28	1993 November 10	NEU	0.44	1993 November 10	NEU	0.44
1991 November 21	EN	0.49	2002 April 03	NEU	0.52	1984 May 27	NEU	0.28	2006 October 13	EN	0.43	2006 October 13	EN	0.43
2009 December 12	EN	0.49	1987 April 12	EN	0.51	1995 May 22	NEU	0.28	2005 October 15	NEU	0.43	2005 October 15	NEU	0.43
2009 February 19	NEU	0.48	1981 February 17	NEU	0.51	2015 June 21	EN	0.27	1997 November 17	EN	0.41	1997 November 17	EN	0.41

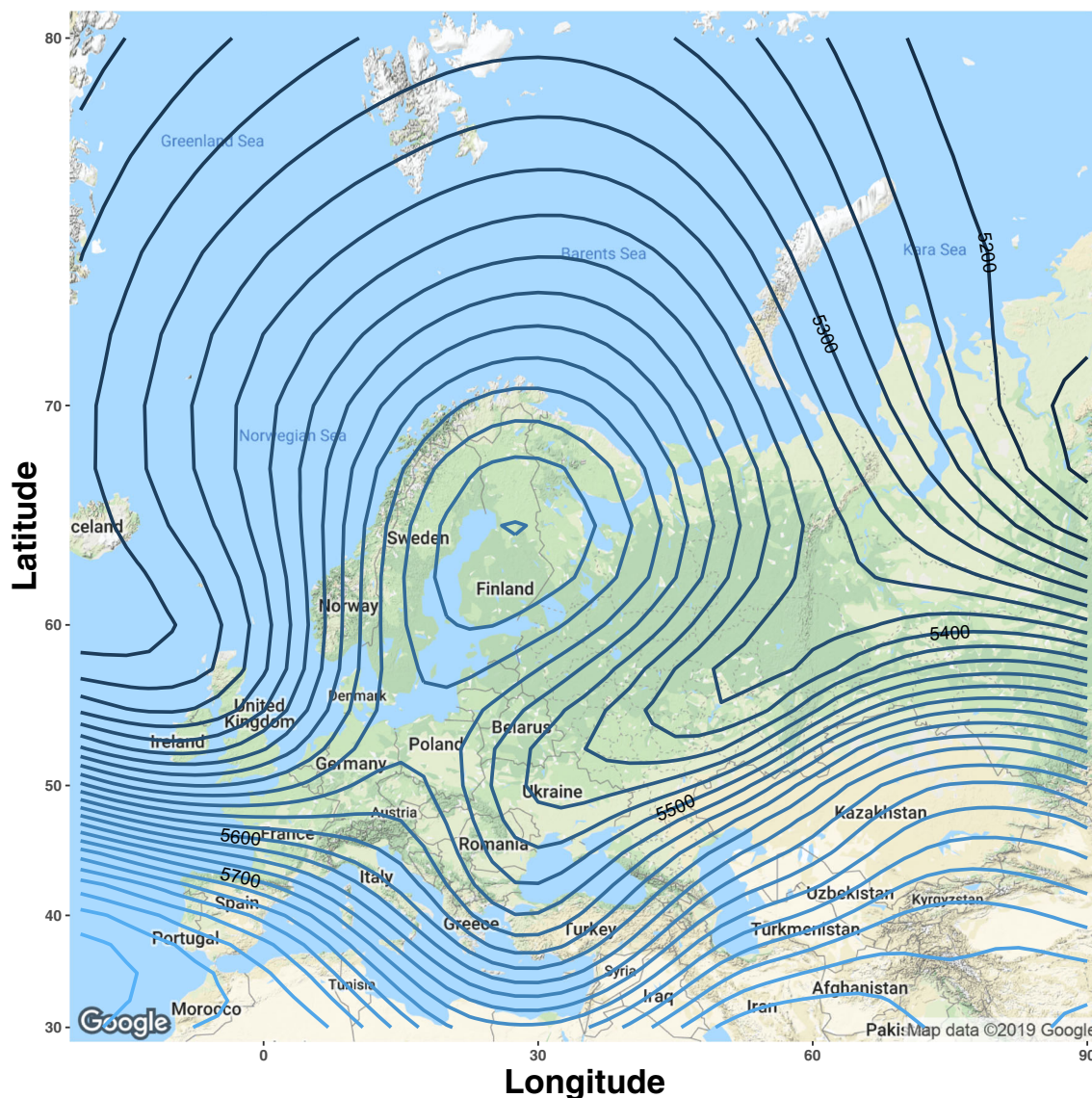


Fig. 15 The composite map of 500 hPa geopotential height (m) for 31 October to 5 November 2009 for the blocking event with the greatest MPF

the Mediterranean coastline and in several cities located in the South Anatolia Region. Rize, Giresun, and Ordu are the cities that observed the highest MPF with values of 0.43, 0.39, and 0.36, respectively. For nonblocked days, MPF ranges between 0.12 and 0.38 nationwide. Similar to the blocked days, the Black Sea coastline and the northeast part of the Marmara Region have the highest MPF. Rize, Giresun, and Ordu are the cities that observed the highest MPF with values of 0.38, 0.32, and 0.29, respectively. These results here demonstrated that blocking increases the MPF across the country. The change in MPF ranges from 12 to 42% in Turkey. The inner part of Anatolia had greater increases in MPF as opposed to the western Black Sea region that observed the lowest values.

The MPF distribution with respect to season showed that winter had the highest values across the country and the mean was 0.31 during blocked days. The average MPF during

blocked days was 0.29, 0.13, and 0.21 in spring, summer, and fall, respectively. The Black Sea Region observed the highest MPF values for all seasons, particularly the city of Rize, which always observed one of the top 3 MPF values in any category. During nonblocked days, the mean MPF values show a similar pattern to the blocked days' MPF values, but with lower values. The winter and spring seasons had similar MPF values, 0.26 and 0.24, respectively. The summer season observed the minimum MPF value of 0.09. For the fall season, the mean MPF was 0.16. The ratio of MPF for blocked days to nonblocked days in the entire dataset and across Turkey explicitly showed that MPF increased during the blocked days. The average change across Turkey was 19, 19, 60, and 28% during the winter, spring, summer, and fall seasons, respectively. The higher summer season MPF ratios were due to smaller values for both blocked and nonblocked days.

In order to investigate whether the location of the block center influenced MPF, the study area was divided into four sectors. The first and the second sector observed the greatest MPF values at 0.25 and 0.27, respectively. The third sector and the fourth sector observed MPF values of 0.22 and 0.21, respectively. When blocking was located in the first and second sectors, Turkey was located on the downstream flank of blocking events, whereas it is located on the upstream flank when blocking was centered in the remaining sectors. Rimbu et al. (2015) found that extreme precipitation events were related to blocking activity within the 0° – 70° E sector, which covers the second, third, and parts of the fourth sector defined here. Huang et al. (2019) indicated that 77% of extreme precipitation events over China are preceded by European blocking events.

In Turkey, there was no relationship between blocking duration and MPF or blocking extent and MPF for the entire dataset in any season or any phase of ENSO. Also, there was no relationship between BI and MPF during the winter and spring seasons for the entire dataset. However, for the summer season, the correlation coefficient was 0.35 and 0.50 for the entire dataset and during NEU years, respectively. Additionally, for the fall season, BI was correlated ($CC = 0.43$ —significant at the 95% level) with MPF in the dataset as well as during NEU years ($CC = 0.48$ —significant at the 95% level).

When examining the 10 wettest MPF blocking events during the study period, it was shown that the blocking center was located in the first and the second sector during all seasons. Their mean BI values were 2.81, 2.23, 2.34, and 2.81 for winter, spring, summer, and fall season events, respectively. Omega-type blocking was observed during cold season events, whereas no particular type of blocking was observed during warm seasons. The average wind was westerly during the 10 wettest events for any season and the wind speed was larger for the wet events than during the driest events as inferred using the geostrophic relationship. When the 850-hPa charts were examined, there was specific humidity advection out of the Mediterranean during wet events for all seasons. There was a tendency toward greater LN occurrence when examining the 10 events with the highest MPF during winter, while there was a tendency toward greater EN occurrence for both the spring and summer seasons. There is no tendency for fall. Nunes et al. (2017) found a tendency toward a greater LN occurrence of extreme precipitation events during winter over southwest Russia. This region is about 1200 km north of Turkey across the Black Sea. They also found a tendency for El Niño season summer and fall extreme precipitation events.

The blocking event associated with the greatest MPF was also examined. The event took place between 31 October 2009 and 5 November 2009. This event was associated with a nationwide MPF of 0.73 and mean total

precipitation of 63.4 mm. The BI was 2.52 and the longitudinal extent was 20° . During this event, heavy rainfall and flash flood events were observed in some cities located in Turkey. In order to understand the influence of blocking as related to extreme precipitation events, a detailed study similar to Nunes et al. (2017) should be performed in the future. Finally, operational forecasters or policy makers should use the results gained here as guidance when blocking is anticipated in short-range or long-range forecasts.

Acknowledgments The authors would like to thank the anonymous reviewers for their time and effort in making this work a stronger contribution.

Funding information We thank the Turkish Water Foundation for supporting Bahtiyar Efe. This work is funded by the Turkish Science Foundation (TUBITAK) with grant number 1059B141700588.

References

- Aalijahan M, Salahi B, Rahimi YG, Asl MF (2018) A new approach in temporal-spatial reconstruction and synoptic analysis of cold waves in the northwest of Iran. *Theor Appl Climatol*. <https://doi.org/10.1007/s00704-018-2601-7>
- Antokhina OY, Antokhin PN, Martynova YV, Mordvinov VI (2016) The impact of atmospheric blocking on spatial distributions of summertime precipitation over Eurasia. *IOP Conf Ser: Earth Environ Sci* 48: 12035. <https://doi.org/10.1088/1755-1315/48/1/012035>
- Baltacı H, Akkoyunlu BO, Tayanç M (2017) Relationship between teleconnection patterns and Turkish climatic extremes. *Theor Appl Climatol* 134:1365–1386. <https://doi.org/10.1007/s00704-017-2350-z>
- Barriopedro D, García-Herrera R, Lupo AR, Hernández E (2006) A climatology of northern hemisphere blocking. *J Clim* 19(6):1042–1063. <https://doi.org/10.1175/JCLI3678.1>
- Bengtsson L (1981) Numerical prediction of atmospheric blocking—a case study. *Tellus* 33(1):19–42. <https://doi.org/10.3402/tellusa.v33i1.10692>
- Bove MC, Elsner JB, Landsea CW, Niu X, O'Brien JJ (1998) Effect of El Niño on U.S. landfalling hurricanes, revisited. *Bull Am Meteorol Soc* 79:2477–2482
- Brunner L, Schaller N, Anstey J, Sillmann J, Steiner AK (2018) Dependence of present and future European temperature extremes on the location of atmospheric blocking. *Geophys Res Lett* 45: 6311–6320. <https://doi.org/10.1029/2018GL077837>
- Demirtaş M (2018) The high-impact 2007 hot summer over Turkey: atmospheric-blocking and heat-wave episodes. *Meteorol Appl* 25: 406–413. <https://doi.org/10.1002/met.1708>
- Gazete Vatan (2009) Yağış nedeniyle bazı seferler iptal!. (Turkish) <http://www.gazetevatan.com/yagis-nedeniyle-bazi-seferler-iptal%2D%2D268162-yasam/>. Accessed 21 Dec 2018
- Huang W, Yang Z, He X, Lin D, Wang B, Wright JS, Chen R, Ma W, Li F (2019) A possible mechanism for the occurrence of wintertime extreme precipitation events over South China. *Clim Dyn* 52:2367–2384. <https://doi.org/10.1007/s00382-018-4262-8>
- Kalnay E, Kanamitsu M, Kistler R, Collins W, Deaven D, Gandin L, Iredell M, Saha S, White G, Woollen J, Zhu Y, Leetmaa A, Reynolds R, Chelliah M, Ebisuzaki W, Higgins W, Janowiak J, Mo KC, Ropelewski C, Wang J, Jenne R, Joseph D (1996) The

- NCEP/NCAR 40-year reanalysis project. *Bull Am Meteorol Soc* 77: 437–471
- Khodayar S, Kalthoff N, Kottmeier C (2018) Atmospheric conditions associated with heavy precipitation events in comparison to seasonal means in the western Mediterranean region. *Clim Dyn* 51:951–967. <https://doi.org/10.1007/s00382-016-3058-y>
- Kömüştü AÜ, Çelik S (2013) Analysis of the Marmara flood in Turkey, 7–10 September 2009: an assessment from hydrometeorological perspective. *Nat Hazards* 66:781–808. <https://doi.org/10.1007/s11069-012-0521-x>
- Lejenas H, Okland H (1983) Characteristics of Northern Hemisphere blocking as determined from a long time series of observational data. *Tellus A* 35(5):350–362. <https://doi.org/10.3402/tellusa.v35i5.11446>
- Lhotka O, Kysely J, Plavcová E (2018) Evaluation of major heat waves' mechanisms in EURO-CORDEX RCMs over Central Europe. *Clim Dyn* 50:4249–4262. <https://doi.org/10.1007/s00382-017-3873-9>
- Luo D, Lupo AR, Wan H (2007a) Dynamics of eddy-driven low-frequency dipole modes. Part I: a simple model of North Atlantic oscillations. *J Atmos Sci* 64:3–28. <https://doi.org/10.1175/JAS3818.1>
- Luo D, Gong T, Lupo AR (2007b) Dynamics of eddy-driven low-frequency dipole modes. Part II: mode characteristics of NAO and diagnostic study. *J Atmos Sci* 64:29–51. <https://doi.org/10.1175/JAS3820.1>
- Lupo AR, Smith PJ (1995) Climatological features of blocking anticyclones in the Northern Hemisphere. *Tellus A* 47(4):439–456. <https://doi.org/10.1034/j.1600-0870.1995.t01-3-00004.x>
- Lupo AR, Jensen AD, Mokhov II, Akperov MG (2017) Changes in blocking characteristics during the first part of the 21st century. *Proceedings* 2017(1):679. <https://doi.org/10.3390/ecas2017-04154>
- Matsueda M (2011) Predictability of Euro-Russian blocking in summer of 2010. *Geophys Res Lett* 38:L06801. <https://doi.org/10.1029/2010GL046557>
- Mokhov II, Timazhev AV, Lupo AR (2014) Changes in atmospheric blocking characteristics within Euro-Atlantic region and Northern Hemisphere as a whole in the 21st century from model simulations using RCP anthropogenic scenarios. *Glob Planet Chang* 122:265–270. <https://doi.org/10.1016/j.gloplacha.2014.09.004>
- NTV (2009) Precipitation, flood, cold!. (Turkish) https://www.ntv.com.tr/galeri/turkiye/etkili-yagis-sel-soguk,4Kdy6v3fXkagcL9Iv9BINg/Hc1gAa7_102QpS4ONJrTHw. Accessed 21 Dec 2018
- Nunes MJ, Lupo AR, Lebedeva MG, Chendeve YG, Solovyov AB (2017) The occurrence of extreme monthly temperatures and precipitation in two global regions. *Pap Appl Geogr* 3:143–156. <https://doi.org/10.1080/23754931.2017.1286253>
- O'Reilly CH, Minobe S, Kuwano-Yoshida A (2016) The influence of the gulf stream on wintertime European blocking. *Clim Dyn* 47:1545–1567. <https://doi.org/10.1007/s00382-015-2919-0>
- Pearson K (1896) Mathematical contributions to the theory of evolution. III. Regression, heredity, and Panmixia. *Philos Trans R Soc London Ser A* 187:253–318
- R Core Team (2018) R: a language and environment for statistical computing. R Foundation for Statistical Computing, Vienna Retrieved <https://www.R-project.org/>. Accessed 15 Dec 2018
- Rabinowitz JL, Lupo AR, Guinan PE (2018, 2018) Evaluating linkages between atmospheric blocking patterns and heavy rainfall events across the north-central Mississippi River valley for different ENSO phases. *Adv Meteorol Article ID* 1217830
- Rimbu N, Stefan S, Busuioc A, Georgescu F (2015) Links between blocking circulation and precipitation extremes over Romania in summer. *Int J Climatol* 36(1):369–376. <https://doi.org/10.1002/joc.4353>
- Scherrer SC, Croci-Maspoli M, Schwierz C, Appenzeller C (2006) Two-dimensional indices of atmospheric blocking and their statistical relationship with winter climate patterns in the Euro-Atlantic region. *Int J Climatol* 26(2):233–249
- Shabbar A, Huang J, Higuchi K (2001) The relationship between the wintertime North Atlantic oscillation and blocking episodes in the North Atlantic. *Int J Climatol* 21(3):355–369. <https://doi.org/10.1002/joc.612>
- Sirdas SA, Özdemir ET, Sezen İ, Efe B, Kumar V (2017) Devastating extreme Mediterranean cyclone's impacts in Turkey. *Nat Hazards* 87:255–286. <https://doi.org/10.1007/s11069-017-2762-1>
- Sitnov SA, Mokhov II, Lupo AR (2014) Evolution of the water vapor plume over Eastern Europe during summer 2010 atmospheric blocking. *Adv Meteorol* 2014:1–11. <https://doi.org/10.1155/2014/253953>
- Sitnov SA, Mokhov II, Lupo AR (2017) Ozone, water vapor, and temperature anomalies associated with atmospheric blocking events over Eastern Europe in spring - summer 2010. *Atmos Environ* 164:180–194. <https://doi.org/10.1016/j.atmosenv.2017.06.004>
- Sousa PM, Trigo RM, Barriopedro D, Soares PMM, Ramos AM, Liberato MLR (2017a) Responses of European precipitation distributions and regimes to different blocking locations. *Clim Dyn* 48(3): 1141–1160. <https://doi.org/10.1007/s00382-016-3132-5>
- Sousa PM, Trigo RM, Barriopedro D, Soares PMM, Santos JA (2017b) European temperature responses to blocking and ridge regional patterns. *Clim Dyn* 50(1–2):457–477. <https://doi.org/10.1007/s00382-017-3620-2>
- Takvim (2009) Urfa'nın etrafi sel!. (Turkish) https://www.takvim.com.tr/yasam/2009/10/31/urfanin_etrafi_sel. Accessed 21 Dec 2018
- Tayanç M, Karaca M, Dalfes HN (1998) March 1987 cyclone (blizzard) over the eastern Mediterranean and Balkan region associated with blocking. *Mon Weather Rev* 126(11):3036–3047. [https://doi.org/10.1175/15200493\(1998\)126%3C3036:MCBOTE%3E2.0.CO;2](https://doi.org/10.1175/15200493(1998)126%3C3036:MCBOTE%3E2.0.CO;2)
- Tibaldi S, Molteni F (1990) On the operational predictability of blocking. *Tellus A* 42(3):343–365
- Treidl RA, Birch EC, Sajecki P (1981) Blocking action in the Northern Hemisphere: a climatological study. *Atmosphere-Ocean* 19(1):1–23. <https://doi.org/10.1080/07055900.1981.9649096>
- Türkeş M, Erlat E (2005) Climatological responses of winter precipitation in Turkey to variability of the North Atlantic Oscillation during the period 1930–2001. *Theor Appl Climatol* 81:45–69. <https://doi.org/10.1007/s00704-004-0084-1>
- Whan K, Zwiers F, Sillmann J (2016) The influence of atmospheric blocking on extreme winter minimum temperatures in North America. *J Clim* 29(12):4361–4381. <https://doi.org/10.1175/JCLI-D-15-0493.1>
- Wickham H (2016) ggplot2: elegant graphics for data analysis. Springer, New York Retrieved <http://ggplot2.org>. Accessed 15 Dec 2018
- Wickham H, François R, Henry L, Müller K (2018) Dplyr: a grammar of data manipulation. Retrieved <https://cran.r-project.org/package=dplyr>. Accessed 15 Dec 2018
- Wiedenmann JM, Lupo AR, Mokhov II, Tikhonova EA (2002) The climatology of blocking anticyclones for the Northern and Southern Hemispheres: block intensity as a diagnostic. *J Clim* 15(23):3459–3473. [https://doi.org/10.1175/1520-0442\(2002\)015<3459:TCOBAF>2.0.CO;2](https://doi.org/10.1175/1520-0442(2002)015<3459:TCOBAF>2.0.CO;2)

Publisher's note Springer Nature remains neutral with regard to jurisdictional claims in published maps and institutional affiliations.